Geochemistry Geophysics Geosystems G3

Article
Volume 12, Number 1
29 January 2011
Q01007, doi:10.1029/2010GC003290
ISSN: 1525-2027

Published by AGU and the Geochemical Society

Lateral, radial, and temporal variations in upper mantle viscosity and rheology under Scandinavia

Auke Barnhoorn
Faculty of Geosciences, Department of Earth Sciences, Utrecht University, Budapestlaan 4, NL-3584 CD Utrecht, Netherlands (auke.barnhoorn@geo.uu.nl)

Wouter van der Wal
Faculty of Geosciences, Department of Earth Sciences, Utrecht University, Budapestlaan 4, NL-3584 CD Utrecht, Netherlands

Faculty of Aerospace Engineering, Delft University of Technology, Kluyverweg 1, NL-2629 HS Delft, Netherlands

Bert L. A. Vermeersen
Faculty of Aerospace Engineering, Delft University of Technology, Kluyverweg 1, NL-2629 HS Delft, Netherlands

Martyn R. Drury
Faculty of Geosciences, Department of Earth Sciences, Utrecht University, Budapestlaan 4, NL-3584 CD Utrecht, Netherlands

[1] The viscosity of the upper mantle has a large control on the dynamics of plate tectonic processes or the response of the Earth's crust after a period of glaciation. Temperature variations within the upper mantle, time-dependent stress changes due to glaciations, and/or variations in the microstructural characteristics of upper mantle rocks (grain size, water content) will result in orders of magnitude variations in upper mantle viscosity. In this study we have taken a microphysical approach to determine variations in viscosity under Scandinavia. We combined experimentally determined flow laws for olivine, data on olivine grain size from Scandinavian xenoliths and peridotites, and stress changes within the upper mantle over the last glaciation period (30 kyr B.P.–present) with two data sets of the temperature distribution within the upper mantle under Europe from Goes et al. (2000) derived from seismic tomography and Artemieva (2006) derived from heat flow measurements. Modeling of olivine viscosity under Scandinavia shows large lateral, radial, and temporal variations in upper mantle viscosity. Lateral temperature variations cause up to four orders of magnitude lateral viscosity variations. Glaciation-induced time-dependent changes of stress cause two orders of magnitude variations in viscosity. Mean viscosity values for a dry upper mantle under Scandinavia are expected to be larger than 10^{22} Pa s, whereas for a wet upper mantle lower viscosity values in the range of 10^{19}–10^{22} Pa s are predicted. Estimates of the upper mantle viscosity under Scandinavia from glacial isostatic adjustment studies (10^{20}–10^{21} Pa s) would indicate that a wet upper mantle below Scandinavia is most likely present. The viscosity modeling furthermore shows that the type of rheology of the upper mantle (linear versus nonlinear rheology) is very sensitive to the microstructural state of the upper mantle. Both mechanisms are active in the upper mantle under Scandinavia on timescales of glacial isostatic adjustment, and their relative contribution varies radially, laterally, and temporally.

Components: 10,100 words, 10 figures, 1 table.

Keywords: upper mantle; rheology; glacial isostatic adjustment; viscosity; microstructure.

Index Terms: 1236 Geodesy and Gravity: Rheology of the lithosphere and mantle (7218, 8160); 3902 Mineral Physics: Creep and deformation; 5120 Physical Properties of Rocks: Plasticity, diffusion, and creep.

Received 7 July 2010; **Revised** 2 December 2010; **Accepted** 14 December 2010; **Published** 29 January 2011.

Barnhoorn, A., W. van der Wal, B. L. A. Vermeersen, and M. R. Drury (2011), Lateral, radial, and temporal variations in upper mantle viscosity and rheology under Scandinavia, *Geochem. Geophys. Geosyst.*, *12*, Q01007, doi:10.1029/2010GC003290.

1. Introduction

[2] Deformation in the upper mantle influences a large variety of processes active in the Earth (convection, subduction, earthquake generation and glacial isostatic adjustment) and is responsible for geophysical signatures in the mantle such as seismic wave speeds, seismic anisotropy or attenuation. The pattern of convective flow, which is controlled by the viscosity structure of the mantle, strongly affects plate velocities, deep-earthquake source mechanisms, the stress distribution in subduction zones and geochemical mixing timescales. During glacial isostatic adjustment (GIA), the viscosity profile of the upper mantle is one of the key parameters controlling the magnitude of uplift and sea level changes as well as the timescale of isostatic adjustment.

[3] Physical conditions within the Earth (temperature, pressure, stress) and microstructural characteristics of the mantle rocks (grain size, presence of water or melt) determine the strength variations and rheological characteristics of the upper mantle. Lateral and radial variations of physical conditions within the Earth or variations in microstructural characteristics of upper mantle rocks can produce large radial and lateral variations in upper mantle viscosity. Lateral variations in upper mantle viscosity affect glacial isostatic adjustment and recently lateral variations in viscosity are incorporated in glacial isostatic adjustment models [*Wu and van der Wal*, 2003; *Zhong et al.*, 2003; *Latychev et al.*, 2005]. Lateral viscosity variations are usually calculated based on a scaling relationship between shear wave velocity data and density [*Ivins and Sammis*, 1995] and relating the density differences to thermal expansion by a depth-dependent thermal expansion coefficient [*Latychev et al.*, 2005; *Paulson et al.*, 2005; *Wang and Wu*, 2006; *Steffen et al.*, 2006]. The disadvantages of such a scaling law are that it assumes one dominant deformation mechanism, neglects pressure dependence and neglects local variations in parameters such as grain size. Contribution of chemical heterogeneities to seismic velocity anomalies can be included [*Shapiro and Ritzwoller*, 2004], or it can be neglected [*Ivins and Sammis*, 1995]. The compositional effect on seismic velocities is small compared to the thermal effect [*Goes et al.*, 2000]. Temperature profiles from *Leitch and Yuen* [1989] used by *Steffen et al.* [2006] and *Wang and Wu* [2006] may underestimate lateral variations in temperature. *Schotman et al.* [2009] use temperature estimates to determine viscosities by solving the heat conduction equation, but they use only three regimes of heat flow data to calculate temperature/viscosity changes with depth.

[4] In this study we use existing estimates of the temperature distribution of the shallow part of the upper mantle to determine the upper mantle viscosity under Scandinavia using a microphysical approach. Rheological flow laws for the main upper mantle mineral olivine [*Hirth and Kohlstedt*, 2003] are combined with the temperature distribution within the upper mantle at different depths [*Goes et al.*, 2000; *Artemieva*, 2006], the stress distribution within the upper mantle and information on the possible grain size of olivine in the mantle from xenoliths [*Kukkonen and Peltonen*, 1999] and peridotite bodies. This approach is similar to that of *Schotman et al.* [2009] except that we take into account the combination of dislocation and diffusion creep, and we use local information for the grain size and temperature. Consideration of grain size is also an important improvement over the relations between temperature and viscosity discussed before.

2. Physical Data Sets for the Upper Mantle and Olivine Viscosity Modeling

2.1. Temperature Distribution Under Scandinavia

[5] Estimates of the temperature distribution in the upper mantle are scarce, yet the temperature distri-

bution has a first-order influence on mantle strength, deformation rate, activity of the different deformation mechanisms and the flow pattern in the mantle. Temperature/depth estimates obtained from geothermobarometry calculations of mantle rocks [e.g., *Brey and Köhler*, 1990; *Franz et al.*, 1996] give some constraint on the temperature conditions in the upper mantle/lithosphere. Modeling studies of different geothermal gradients within the Earth can also provide estimates of the temperature in the upper mantle, such as by modeling of an age-dependent oceanic lithosphere [*Turcotte and Schubert*, 2002]. However, both xenolith data and geothermal gradients only provide one-dimensional isolated temperature data sets and do not provide detailed information on lateral temperature variations within specific regions of the Earth.

[6] Temperature grids derived in two different ways are available for the upper mantle under Europe [*Goes et al.*, 2000; *Artemieva*, 2006]. Both data sets show lateral variations in temperature under Europe with small grid spacings (0.6° × 0.6° for *Goes et al.* [2000]; 1° × 1° for *Artemieva* [2006]) at different depths in the shallow upper mantle (<230 km). *Goes et al.* [2000] inverted P wave seismic tomography data from *Bijwaard et al.* [1998] and S wave seismic tomography data from *Marquering and Snieder* [1996] using experimental data on elastic parameters and anelasticity and a garnet lherzolitic composition of the upper mantle [*Jordan*, 1979]. The temperature under Europe at depths of ~52, 95, 145 and 200 km was produced. It was shown that the variations in P and S wave speeds across Europe were predominantly caused by thermal variations and not by compositional variations of the upper mantle. *Goes et al.* [2000] concluded that the thermal data set is in agreement with existing thermal estimates from heat flow data and the tectonic setting of Europe. The uncertainty in the temperature ranges from 100 to 150°C.

[7] We use the thermal data sets of *Goes et al.* [2000] for Scandinavia (Figure 1) at the four depths in the modeling of upper mantle viscosity. A 2 × 2 running average of the individual temperature data points of *Goes et al.* [2000] was performed to achieve the same grid spacing as the stress grids (see section 2.2) and at the same time to somewhat smooth the temperature data and reduce the effect of some of the outliers in the data set.

[8] The temperature data set of *Artemieva* [2006] is a thermal model for the continental lithosphere based on information of geotherms for continental terranes of different ages which are constrained by borehole heat flow measurements [*Artemieva and Mooney*, 2001]. The data set covers continental Europe, not under the seas or oceans, for depths of 50, 100 and 150 km (Figure 1). Generally, the data set of *Artemieva* [2006] is smoother than the data set of *Goes et al.* [2000] with weaker short-distance lateral variations. Similarities in the thermal structure can be seen between both data sets, such as the relatively low temperatures under the Baltic shield/Finland in comparison with the higher temperatures under southwestern Norway. Locally, temperature differences between both data sets can be up to 500°C (Figure 2a). However, overall, the differences between the data sets are smaller (Figure 2). The data set of *Artemieva* [2006] predicts somewhat lower mean temperatures for Europe and Scandinavia in comparison with the data set of *Goes et al.* [2000], especially at the depths around 50 and 100 km (Figures 2a and 2b). At 150 km depths, the difference in mean temperature between both data sets is smaller (Figure 2b). The higher mean temperatures of *Goes et al.*'s [2000] data set in comparison with the data set of *Artemieva* [2006] can be reconciled in two ways. First, the presence of water in the upper mantle [*Karato*, 2003] or attenuation of seismic waves due to grain size [e.g., *Faul and Jackson*, 2005] has not been taken into account in the conversion from seismic wave speeds to temperature in *Goes et al.*'s [2000] data set. Not taking into account the effects of water and grain size may result in an overestimation of the temperatures potentially explaining the difference in both temperature data sets. Second, borehole heat flow measurements [*Artemieva*, 2006] may only be representative for the crust and shallower part of the upper mantle. Extrapolation of geotherms to larger depths within the upper mantle could potentially result in an underestimation of the mantle temperatures.

[9] The approaches of *Goes et al.* [2000] of inversion of P and S seismic tomography data and *Artemieva* [2006] using geotherms and borehole heat flow data to determine the thermal structure of the upper mantle below Europe are totally different. Similarities and differences in temperature between the data sets occur and they have an effect on the viscosity modeling of the upper mantle. The viscosity results using both data sets show similar sensitivities of the dominant deformation mechanisms on the upper mantle grain size and therefore can be used to discuss the likely type of viscous flow present in the upper mantle. The results also give restrictions on the range of viscosities expected to be present in the upper mantle.

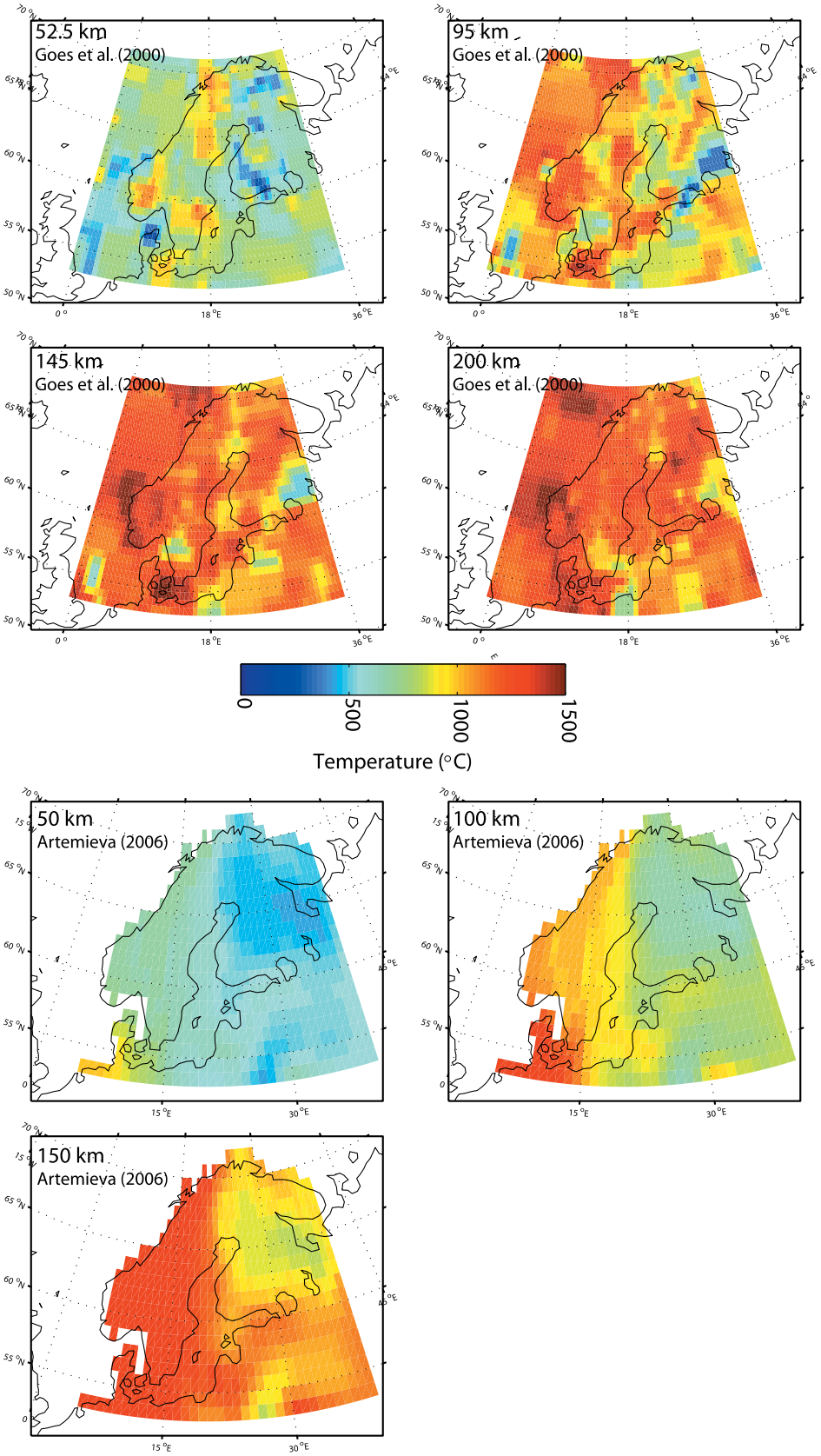

Figure 1. Upper mantle temperature distribution under Scandinavia (first four panels) from *Goes et al.* [2000] at 52.5, 95, 145, and 200 km depths and (last three panels) from *Artemieva* [2006] at 50, 100, and 150 km depths.

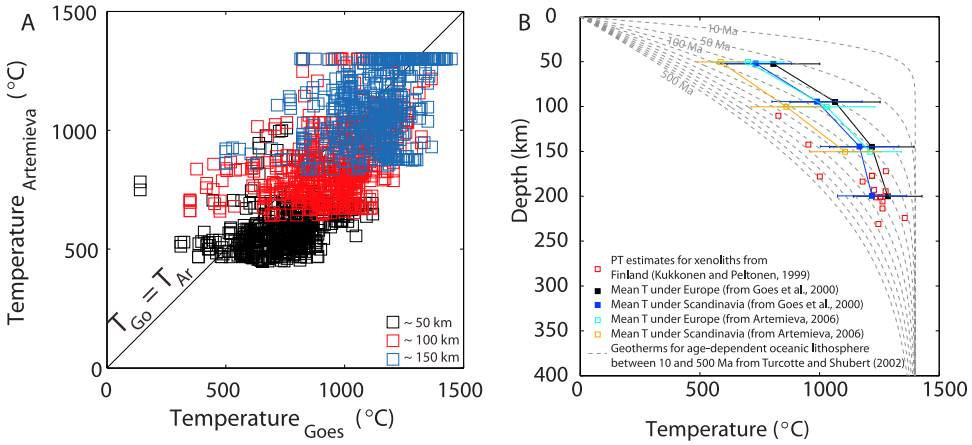

Figure 2. (a) Comparison of temperature estimates of *Goes et al.* [2000] and *Artemieva* [2006] for all locations under Scandinavia at depths of ~50, 100, and 150 km. The data of *Goes et al.* [2000] have been interpolated spatially to correspond to 1° × 1° grid of *Artemieva*'s [2006] data. Temperatures of *Goes et al.* [2000] at depths of 52.5, 95, and 145 km are compared with temperatures of *Artemieva* [2006] at depths of 50, 100, and 145 km without applying a correction for the differences in depth. (b) Mean temperatures under Europe and Scandinavia from temperature data sets of *Goes et al.* [2000] and *Artemieva* [2006]. Pressure-temperature estimates from xenoliths from Finland [*Kukkonen and Peltonen*, 1999] and geotherms for oceanic lithospheres of various ages [*Turcotte and Schubert*, 2002] using a potential temperature of 1400°C are also shown.

2.2. Stress Distribution Under Scandinavia

[10] We have computed a dynamic stress field for Scandinavia from the three-dimensional finite element model for glacial isostatic adjustment of *Schotman et al.* [2009] based on the commercial program Abaqus. The model has a total of 97 × 97 elements in the horizontal direction and 10 element layers in the vertical direction. Elements in the inner surface area of 2920 × 2920 km are 80 × 80 km wide. The top 120 km is taken to be fully elastic. Elastic parameters are obtained from PREM. The model is loaded by the ice model of *Lambeck et al.* [1998] which is mapped to the model grid by a Lambert equal area projection. The rheology is a combination of dislocation and diffusion creep parameters that best fits a global set of historic sea level data [*van der Wal et al.*, 2010]. The relation between stress and strain rate in a uniaxial experiment is taken to be the same as the relation between equivalent stress and equivalent strain rate and the individual components of the stress tensor are assumed to be proportional to the corresponding components of the strain rate tensor [*Ranalli*, 1995]. The GIA model provides the von Mises equivalent stress as output,

$$q = \sqrt{\frac{3}{2}\sigma_{ij}\sigma_{ij}}, \qquad (1)$$

where σ_{ij} is an element of the stress tensor. Von Mises stresses in the upper mantle at depths of 52, 95, 145 and 200 km are calculated for every kyr between 30 kyr and present. Figures 3 and 4a and Animation S1 in the auxiliary material show the von Mises stresses for the four depths (Figure 3 at timesteps 30, 18, 8 and 0 kyr B.P.).[1] The stress field for the upper mantle under Scandinavia is characterized by high stress levels at the two shallow depths (52.5 and 95 km) between 30 kyr B.P. and ~20 kyr B.P. (maximum ice load) followed by a decrease in stress levels toward present. The deeper parts (145 and 200 km) show increased stresses between ~22 kyr B.P. and ~8 kyr B.P. Maximum stress occurs later with increasing depth. This is caused by the delay in propagation of stress toward larger depth in the upper mantle during glacial loading. The computed stress levels in the upper mantle are on average within the range of 1 to several tens of MPa (Figure 4) for mantle convection [e.g., *Schmeling*, 1987; *Ranalli*, 1995; *Steinberger et al.*, 2001] and are close to stress estimates (<3 MPa) for the mantle wedge in subduction zone settings [*Kneller et al.*, 2005]. Plate tectonic stresses and stresses induced by glaciations act simultaneously on the upper mantle under Scandinavia. Both stresses are potentially of the same order of magnitude [*Ranalli*, 1995]. Because the combined effect also depends on direction of each of the stress components [*Schmeling*, 1987] stress invariants cannot simply be added. The GIA model that is used to compute the stress map can-

[1] Auxiliary materials are available in the HTML. doi:10.1029/2010GC003290.

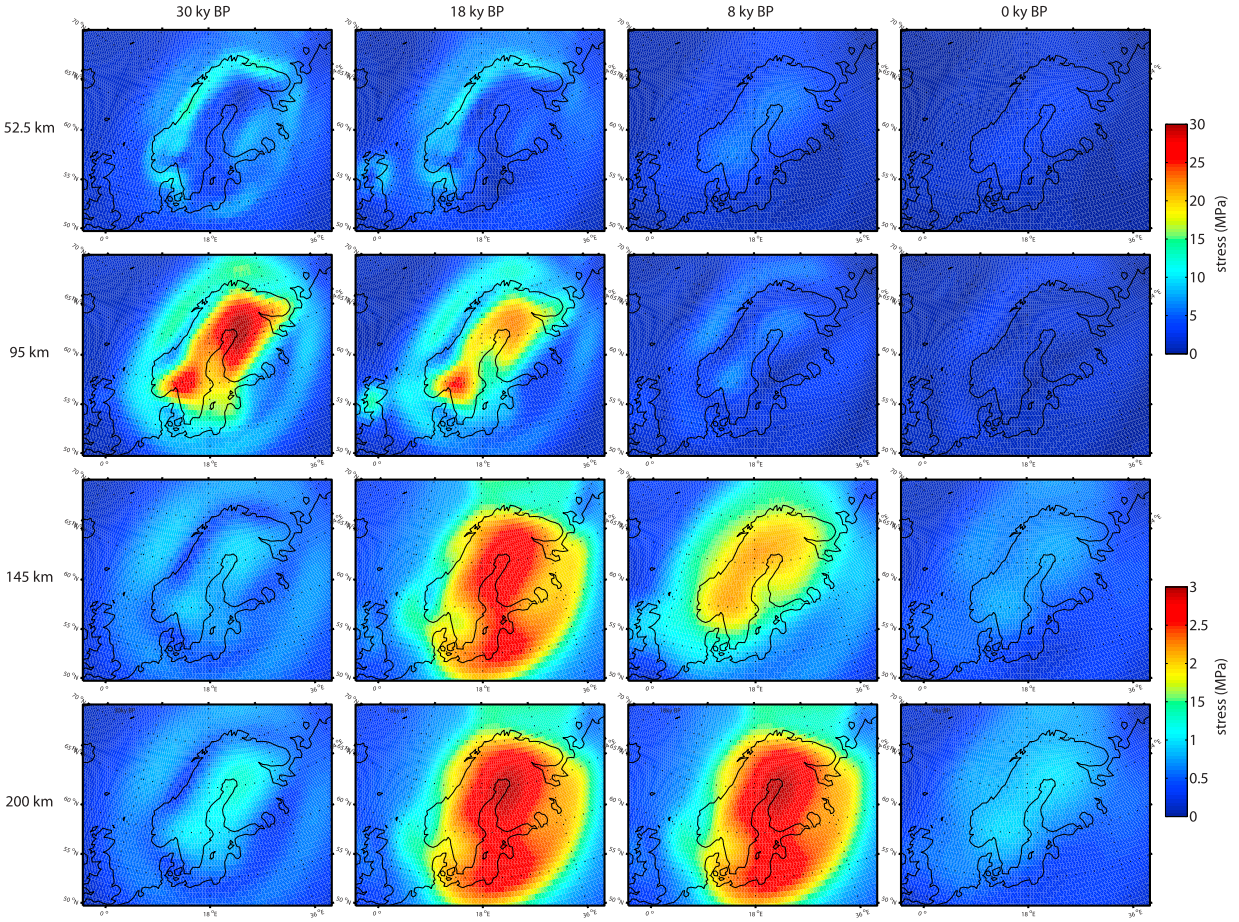

Figure 3. Von Mises stress maps for depths of 52.5, 95, 145, and 200 km at four time intervals (30 kyr B.P., 18 kyr B.P., 8 kyr B.P., and present). Note that the maps for 52.5 and 95 km have a different color scale than the maps for 145 and 200 km depths. The von Mises stress is the equivalent stress multiplied by $\sqrt{3}$.

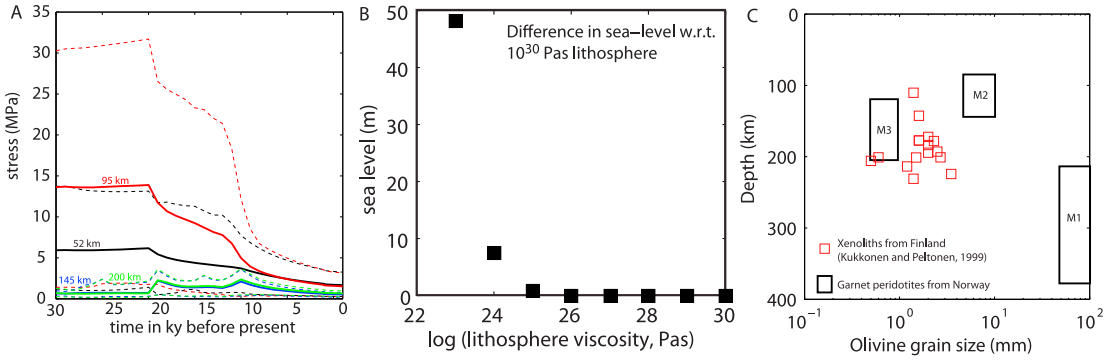

Figure 4. (a) Mean stress (solid lines) changing with time between 30 kyr B.P. and present for depths of 52, 95, 145, and 200 km based on a 3-D finite element model for glacial isostatic adjustment by *Schotman et al.* [2009]. Dotted lines represent 1σ standard deviation of the stress levels for each depth. (b) Viscosity in the top layer of an earth model is varied, and the difference in uplift rate is computed with respect to a top layer that is effectively elastic. It can be seen that if the top layer is 10^{25} Pa s a significant difference in sea level is obtained. (c) Upper mantle grain size estimates from xenoliths from Finland [*Kukkonen and Peltonen*, 1999] and from the garnet peridotites from Norway. Three different mineral assemblages with three different grain sizes occur in those garnet peridotites. M1 corresponds to the oldest and deepest asthenospheric megacryst assemblage with grain sizes >5 cm. M2 corresponds to the Proterozoic lithospheric assemblages with grain sizes around 1 cm, and M3 corresponds to the youngest lithospheric assemblage with grain sizes around 1 mm. The M2 assemblage is by far the most dominant nowadays in the peridotites. M1 and M3 take up <1% in volume of the peridotite bodies exposed.

not account for mantle convection stress, and we have chosen not to add mantle convection stress to the stress map, because magnitudes and directions are not well constrained.

2.3. Possible Grain Sizes Within the Upper Mantle Under Scandinavia

[11] The olivine grain size is an important parameter in the viscosity calculations for the diffusion creep mechanism, since linear viscous diffusion creep flow laws contain a large grain size dependence. Knowledge of grain size in the upper mantle is therefore vital to determine reliable estimates of upper mantle viscosities [e.g., *Mercier et al.*, 1977; *Ave Lallemant et al.*, 1980]. Direct estimates of the grain size in the upper mantle can only come from samples of kimberlite xenoliths or from orogenic peridotite bodies now exposed at the surface of the Earth. In Scandinavia, both types of mantle rocks are present. Olivine-bearing kimberlite xenoliths occur on the Scandinavian Shield in central Finland [*Kukkonen and Peltonen*, 1999] and orogenic peridotite bodies occur in the Western Gneiss Region of Norway [e.g., *van Roermund et al.*, 2000]. Both the Finnish xenoliths and the Norwegian peridotite bodies have exhumed into the crust already in the Paleozoic (530 Ma and ~480–420 Ma ago) and it is therefore uncertain whether the present-day upper mantle has the same olivine grain size as can be observed in the xenoliths and peridotites. Later deformation events (e.g., opening of the Atlantic Ocean, extension of the North Sea graben or uplift due to glaciation events) have mainly affected the margins of the Scandinavian continental crust and are not likely to have significantly altered the cratonic upper mantle microstructures under Scandinavia, as concluded by *Kukkonen and Peltonen* [1999] for the Finnish xenoliths. The deeper parts of the upper mantle were relatively cold during the Caledonian orogeny and experienced no known subsequent pulse of high temperatures limiting the possibility that high-temperature annealing caused a substantial increase in olivine grain size within the upper mantle under Scandinavia. We therefore assume that the microstructure present in the xenoliths and peridotites is still representative of the present-day upper mantle microstructures below Scandinavia.

[12] Geothermobarometry and microstructural analyses of the xenolith samples show that their microstructures have equilibrium assemblages of ~200 km depth and ~1000–1200°C (Figure 4). The olivine grain sizes for those samples vary slightly between 1 and 4 mm [*Kukkonen and Peltonen*, 1999]. Sub-mm olivine grain sizes only occur in two websterite samples (Figure 4) in which olivine is not the dominant constituent.

[13] Another possibility is that the upper mantle grain size more closely resembles the grain sizes observed in the peridotite bodies of the Western Gneiss Region in Norway. Three different grain size assemblages (M1, M2 and M3, Figure 4) are present in those peridotite bodies. The most commonly observed grain size of olivine in the peridotites is around 10 mm in size corresponding to the M2 mineral assemblages. More than 95% of the exposed peridotite bodies have grain sizes belonging to this M2 mineral assemblage. Geochemical analyses and dating of the M2 mineral assemblage shows that this assemblage formed during the Proterozoic at depths of ~120–150 km during the progressive cooling of the lithosphere from temperatures as high as 1800°C [*van Roermund et al.*, 2000]. The largest grain sizes occur in the M1 megacryst assemblages where grain sizes typically larger than a few centimeters to as large as 50 cm occur for olivine, orthopyroxene and garnet. These M1 megacryst grain sizes are remnants of a very early Archean and deep upper mantle (200–400 km) history of the peridotite body [*Spengler et al.*, 2006]. Only remnants (<1%) of the M1 mineral assemblage are still preserved. The M1 grain sizes may be representative for the asthenospheric upper mantle which has been almost completely replaced in the later, more shallow history of the Norwegian peridotites by the Proterozoic M2 lithospheric upper mantle mineral assemblage. A mm-sized (3–4 mm) olivine mineral assemblage (M3) also occurs in the peridotite bodies and is formed during Caledonian (~420 Ma) subduction related deformation [*Spengler et al.*, 2009]. Similarly to the M1 mineral assemblage, the M3 mineral assemblage can also be observed only locally in the peridotite bodies.

[14] Grain size reduction in the upper mantle due to increased stresses during recent glacial isostatic adjustments is unlikely to have occurred. Accumulated strain over the timescales of glacial isostatic adjustments (e.g., 30 kyr) is too small for dynamic recrystallization to occur. Uplift on the order of hundreds of meters over areas of hundreds of kilometers to depths of at least 400 km result locally only in very small strains. The local strain is smaller than the strain needed to reach the onset of recovery processes such dynamic recrystallization. Therefore, grain size changes within the upper mantle during GIA are not expected to occur. Thus, all viscosity variations due to grain size are caused by preexisting heterogeneities in the mantle and are stable (in terms of effect of grain size) during

Table 1. Olivine Flow Law Parameters for a Dry and Wet Upper Mantle From *Hirth and Kohlstedt* [2003]

	A^a	n	p	r	α^b	E (kJ/mol)	V (10^{-6} m^3/mol)	C_{OH}
Dry diffusion	1.5×10^9	1	3	-	30	375	5	0
Wet diffusion	1×10^6	1	3	1	30	335	4	1000
Dry dislocation	1.1×10^5	3.5	0	-	30	530	5	0
Wet dislocation	90	3.5	0	1.2	30	480	11	1000

[a]For stress in MPa, temperature in K, pressure in Pa, C_{OH} in H/10^6 Si, and grain size in μm.
[b]Here $\varphi = 0$ (all modeling is melt-free).

glacial-interglacial cycles. In the upper mantle viscosity modeling two grain size values have been used: (1) a 4 mm grain size representative for the maximum grain size of the mantle xenoliths from Finland as well as the M3 mineral assemblage of the peridotite bodies from Norway and (2) a 10 mm grain size representative for the dominant lithospheric (M2) grain size of the peridotite bodies.

2.4. Olivine Viscosity Modeling

[15] Diffusion and dislocation flow laws for olivine from *Hirth and Kohlstedt* [2003] were used to calculate the viscosity of the upper mantle. The diffusion and dislocation creep flow laws describe the dependence of the strain rate ($\dot{\varepsilon}$) on temperature (T), grain size (d), deviatoric stress (σ), pressure (P), water content (fH_2O or its equivalent C_{OH}) and melt content (φ),

$$\dot{\varepsilon} = A\sigma^n d^{-p} fH_2O^r \exp(\alpha\varphi) \exp\left(\frac{E+PV}{RT}\right), \qquad (2)$$

where A and α are constants, and n, p and r are the stress, grain size and water fugacity exponents, E the activation energy and V the activation volume. We assume that the equivalent stress can be used as the stress parameter in equation (2). The von Mises stress is the equivalent stress multiplied by $\sqrt{3}$.

[16] Values for the flow law parameters for wet and dry dislocation and diffusion creep are given in Table 1. For the modeling of wet upper mantle viscosities a C_{OH} of 1000 H/10^6 Si is taken as the water content in olivine (in a similar manner as *Hirth and Kohlstedt* [2003] in their Table 2) of the upper mantle [*Hirth and Kohlstedt*, 1996]. All modeling is performed with the assumption that melt is absent ($\varphi = 0$). Pressure (P) is calculated as $P = 0.033$ GPa/km. The dislocation creep strain rate ($\dot{\varepsilon}_{disl}$) is typically not dependent on grain size ($p = 0$) and has a large stress exponent ($n = 3.5$), whereas the diffusion creep strain rate ($\dot{\varepsilon}_{diff}$) has a large dependence on grain size ($p = 3$) and linear dependence on stress ($n = 1$). A composite flow law [e.g., *Ranalli*, 1995] in which both dislocation creep and diffusion creep contribute to the deformation is also used,

$$\dot{\varepsilon}_{total} = \dot{\varepsilon}_{diff} + \dot{\varepsilon}_{disl}. \qquad (3)$$

[17] The deformation mechanism that deforms with the fastest strain rate at a given set of conditions of temperature, stress, grain size, melt and water content contributes most to the total strain rate. The dislocation creep flow law and thus also the composite flow law have a nonlinear relation between stress and strain rate and therefore the viscosity estimates (η_{disl} and η_{total}) depend on stress and are usually called effective viscosities. The effective viscosity for diffusion creep, dislocation creep and composite rheology as a function of the von Mises stress q (equation (1)) is

$$\eta_{diff} = \frac{1}{3A^*_{diff} q}; \quad \eta_{disl} = \frac{1}{3A^*_{disl} q^{n-1}}; \quad \eta_{comb} = \frac{1}{3A^*_{diff} q + 3A^*_{disl} q^{n-1}}, \qquad (4)$$

where A^* contains all parameters except for stress in the flow law (equation (2)) determined from uniaxial experiments, and n is the stress exponent. In this study, we refer to effective viscosities when describing the dislocation creep viscosity or total viscosity of the upper mantle.

[18] Our viscosity estimates can only be compared to those derived in glacial isostatic adjustment studies if we use the same definition of the lithosphere as in glacial isostatic adjustment models. The short-term elastic lithosphere is defined as the outer shell that behaves almost entirely elastic on the timescale of glacial isostatic adjustment [*Martinec and Wolf*, 2005]. In order to find a cutoff value of the lithospheric viscosity above which the lithosphere can be considered completely elastic, we perform simulations with the normal mode codes of *Vermeersen and Sabadini* [1997] with the ICE-5G loading history [*Peltier*, 2004] and a uniform layer of water accompanying ice volume change at each time step. Historic sea levels form the most important glacial isostatic adjustment

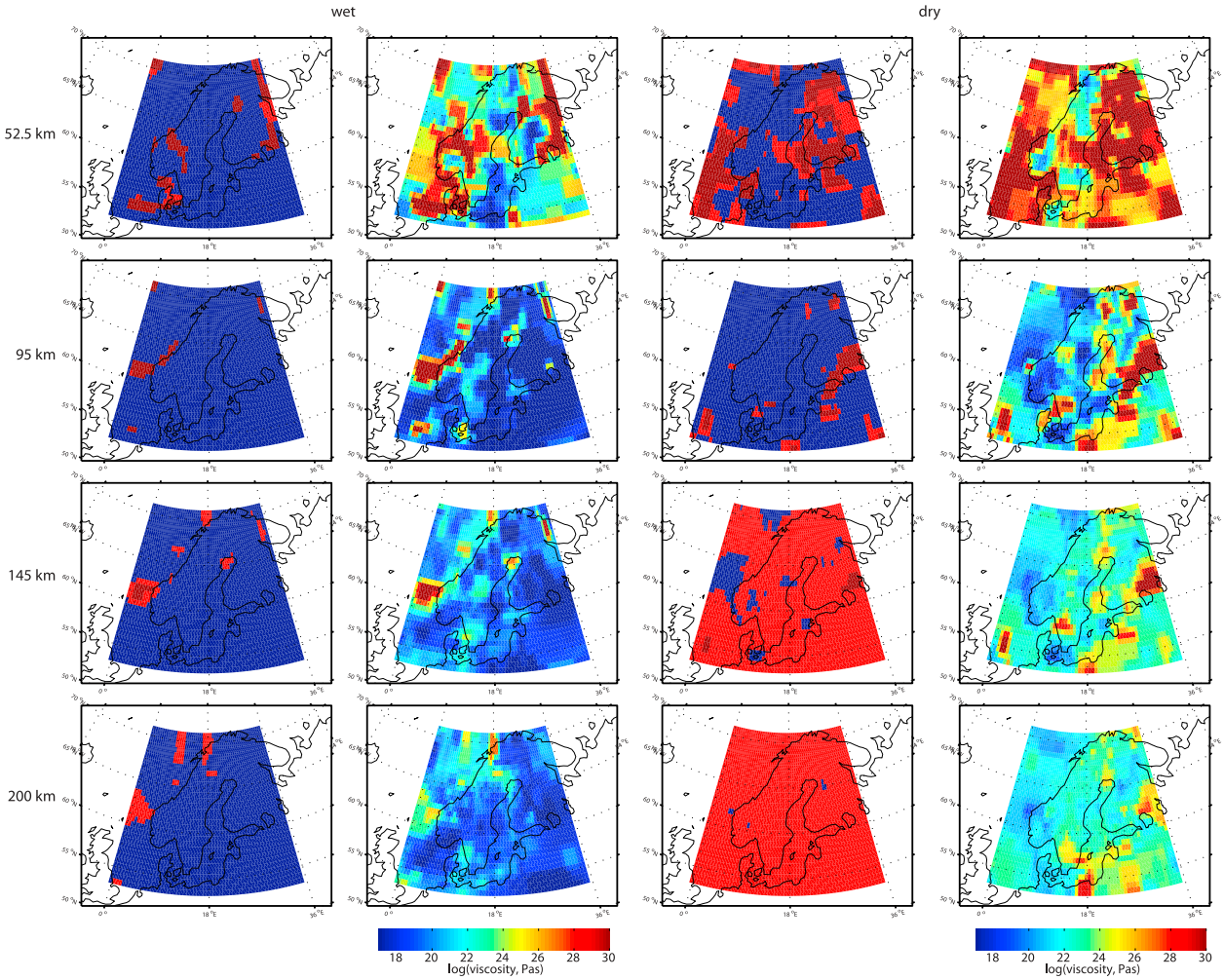

Figure 5. Dominant deformation mechanisms and predicted viscosity under Scandinavia at 30 kyr B.P. in (first two columns) a wet upper mantle and (last two columns) a dry upper mantle and an olivine grain size of 10 mm (based on temperature data set of *Goes et al.* [2000]). Dominant deformation mechanisms (brown indicates $\eta_{total} > 10^{30}$ Pa s; red indicates diffusion creep; blue indicates dislocation creep).

observation, and they have a typical error bar of 1 to 10 m [*Tushingham and Peltier*, 1991]. The viscosity in the lithosphere was lowered from a value of 10^{30} Pa s until 10^{21} and the difference in position of the crust at present is plotted in Figure 4b with respect to that of a purely elastic lithosphere of 10^{30} Pa s. Lowering the viscosity of the lithosphere from 10^{26} to 10^{25} Pa s results in a difference in sea level close to 1 m. We have therefore chosen to use the value of 10^{25} Pa s as a cutoff value for elastic deformation. This somewhat agrees with *Klemann and Wolf* [1998] who find that deformation occurs when the bottom of the lithosphere has a viscosity between 5×10^{24} Pa s and 3×10^{23} Pa s. It is somewhat higher than the cutoff viscosity of 10^{23} Pa s estimate by *Schotman et al.* [2009] which was simply derived from the Maxwell relaxation time for different lithospheric viscosity and rigidity.

3. Results

[19] The lateral variations in temperature at all four depths under Scandinavia are significant. For example, between north Finland and southwest Norway a temperature difference in the order of 250°C is present *Artemieva*'s [2006] data set. *Goes et al.*'s [2000] data set shows even larger variations (up to 500°C) at the shallowest depths of 52 and 95 km, but with much less variation in temperature between north Finland and southwest Norway at the deepest depths of 145 and 200 km. This variation in temperature results in large lateral variations in viscosity under Scandinavia (Figure 5).

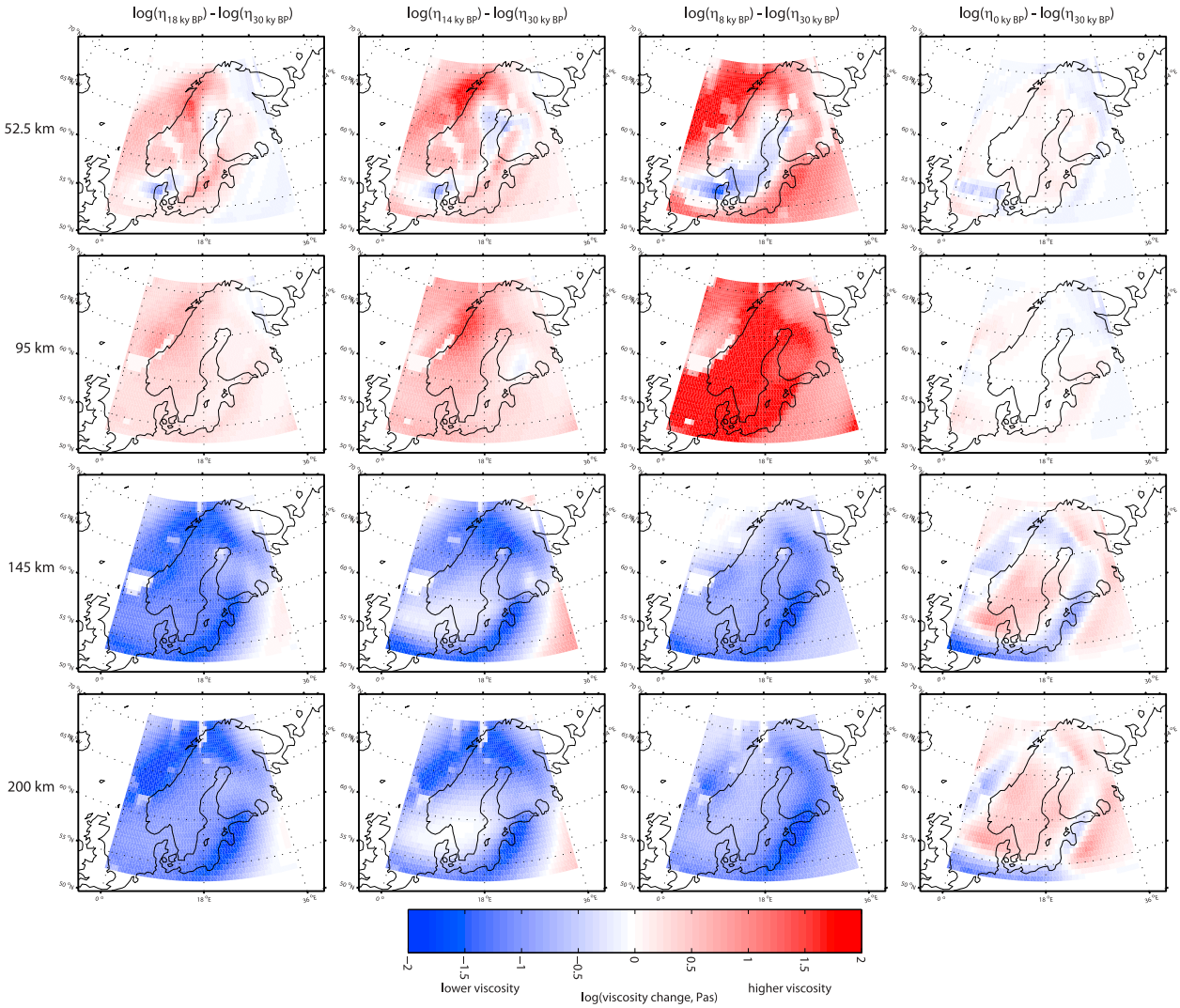

Figure 6. Relative change in viscosity with respect to the viscosity at 30 kyr B.P. in a wet upper mantle for 18 kyr B.P., 14 kyr B.P., 8 kyr B.P., and present. Red indicates an increase in viscosity; blue indicates a decrease in viscosity.

The cold/high viscosity region has a total viscosity which is at least four orders of magnitude higher than the warm/low viscosity region (e.g., Figure 5).

[20] Similarly, a difference in either water content of the upper mantle, stress levels in the upper mantle or olivine grain size influence the upper mantle viscosity values. For both diffusion and dislocation creep mechanisms an increase in water content (e.g., from C_{OH} = 100 to 1000 H/10^6 Si) results in a significant decrease in viscosity. Figure 5 shows that the upper mantle viscosities at e.g., 95 km for a dry (C_{OH} = 0 H/10^6 Si) upper mantle are on average around 2–3 orders of magnitude higher than in a wet upper mantle (C_{OH} = 1000 H/10^6 Si). A change in olivine grain size only affects the regions where diffusion creep is the dominant deformation mechanism, since only diffusion creep flow laws have a grain size dependency in equation (2). Mainly at small grain sizes (d < 10 mm), depending also on the stress levels and water content, significant regions occur in the upper mantle under Scandinavia where diffusion creep is the dominant deformation mechanism. In those regions viscosity is affected significantly by grain size. On the other hand, stress levels have a strong control on the viscosity in regions where dislocation creep is the dominant deformation mechanism due to the stronger stress dependency of dislocation creep flow laws in comparison with diffusion creep flow laws (n = 3.5 versus n = 1). Dislocation creep mechanisms are only dominant in a dry upper mantle at relatively large grain sizes ($d \geq$ 10 mm, see Figure 5), but in a wet upper mantle dislocation creep mechanisms are

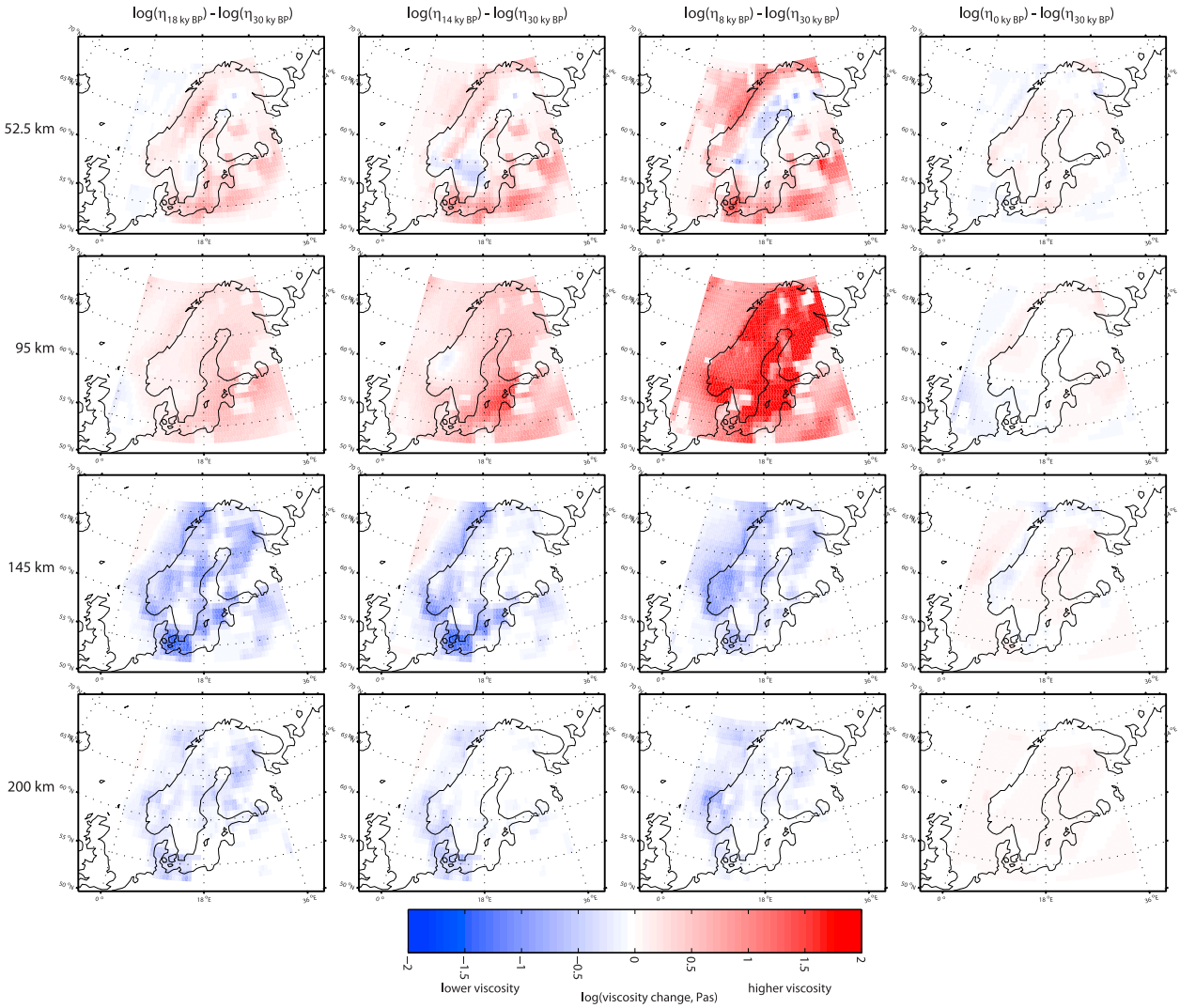

Figure 7. Relative change in viscosity (logarithm) with respect to the viscosity at 30 kyr B.P. in a dry upper mantle for 18 kyr B.P., 14 kyr B.P., 8 kyr B.P., and present.

predicted to dominate the deformation already at much smaller grain sizes. Time-dependent changes of viscosity caused by the time-dependent changes of stress (Figure 3) are thus much larger in a dislocation creep-dominated wet upper mantle than in a more diffusion creep-dominated dry upper mantle (Figures 6 and 7 and Animations S2 and S3). The viscosity changes due to changes in stress with time are at least two orders of magnitude large, with mainly an increase in viscosity from 30 kyr B.P. in the lithosphere or the shallow upper mantle (52 and 95 km depth) and both a decrease followed by an increase in viscosity occurring in the deeper levels of the upper mantle (145 and 200 km, Figures 6–8). The time-dependent changes of viscosity become more complicated when certain regions undergo a change of deformation mechanism with time. A change from dislocation creep to diffusion causes a stable viscosity with time despite fluctuations in stress level, while a change from diffusion creep to dislocation creep causes sudden time/stress-dependent viscosities. Time-dependent changes in deformation mechanism would also complicate the viscosity patterns when the upper mantle has a heterogeneous distribution of grain size. A dislocation creep dominated mantle results in a homogeneous viscosity distribution, while a diffusion creep dominated mantle results in a strongly heterogeneous viscosity distribution. Time-dependent changes of stress and in dominance of deformation mechanism may thus cause significant changes in the viscosity distribution of the upper mantle during glacial isostatic adjustment. The variation in dominance of one of the two deformation mechanisms (dislocation

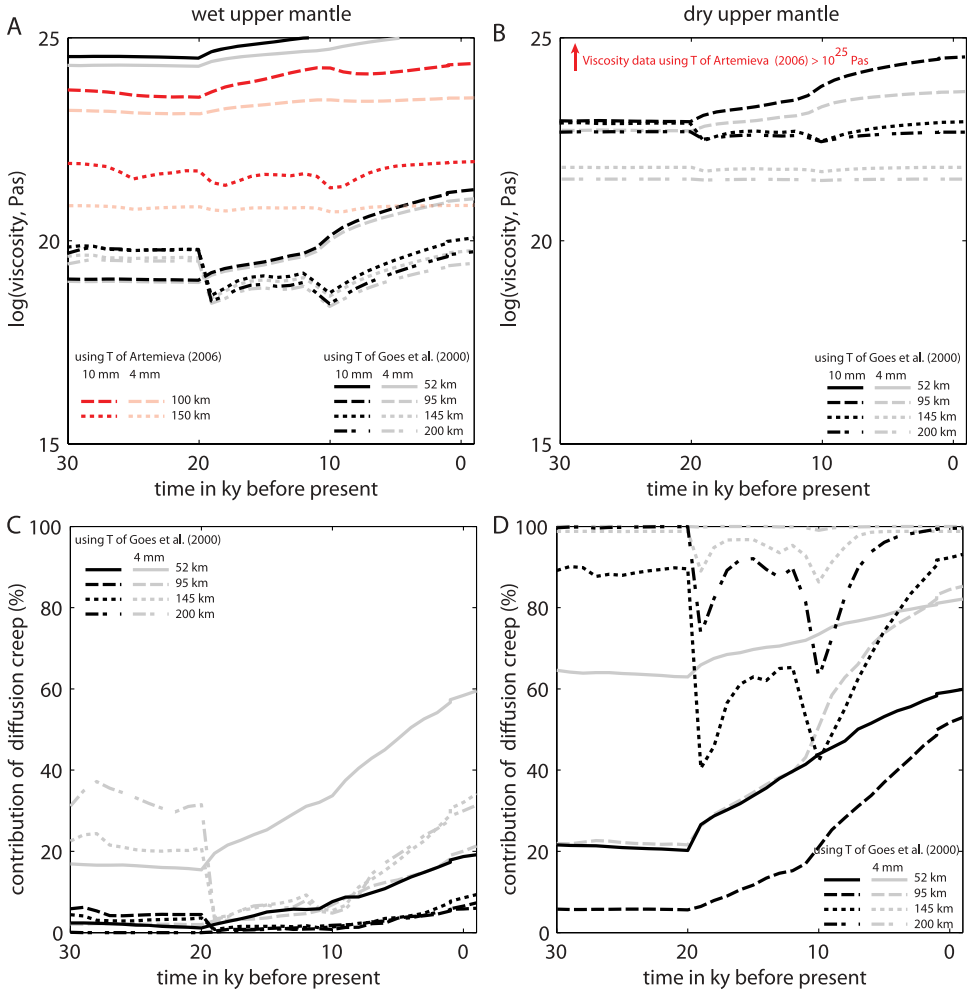

Figure 8. (a and b) Time-dependent variations in mean viscosity (logarithm) under Scandinavia for a wet (Figure 8a) and dry (Figure 8b) upper mantle. All viscosities at each depth for Scandinavia are averaged to obtain a mean viscosity for that depth. Black lines are based on the temperature data of *Goes et al.* [2000]; red lines are based on the temperature data of *Artemieva* [2006]. In a dry upper mantle the temperature data of *Artemieva* [2006] predict mean viscosities in excess of 10^{25} Pa s for each depth. (c and d) Contribution of diffusion creep between 0 and 100% to the total deformation for each time step in a wet (Figure 8c) and dry (Figure 8d) upper mantle based on the temperature data of *Goes et al.* [2000].

creep and diffusion creep) with grain size, stress level and water content for the temperature conditions of the Scandinavian upper mantle shows that it is likely that both deformation mechanisms are active in the upper mantle. This finding is in contrast to *Schotman et al.* [2009] who found that dislocation creep is not likely to occur because it leads to too high upper mantle viscosities.

[21] The base 10 logarithm of the viscosities estimates for the upper mantle under Scandinavia are averaged for each depth to represent the Scandinavian upper mantle with one mean viscosity value for each time step between 30 kyr B.P. and present (Figures 8a and 8b). Mean total viscosity values for a dry upper mantle and a grain size of 4 or 10 mm using the temperature data set of *Goes et al.* [2000] vary between 10^{22} and 10^{25} Pa s at depths of 95, 145 and 200 km, whereas the data set of *Artemieva* [2006] predicts mean viscosities mostly larger than 10^{25} Pa s for a dry upper mantle (Figure 8b). In a wet upper mantle (Figure 8a) mean total viscosity values are expected to be around 10^{18}–10^{22} Pa s at depths ≥ 95 km using *Goes et al.* [2000] and 10^{21}–10^{24} Pa s for depths of 100–150 km using *Artemieva* [2006]. Mean viscosities in a wet upper mantle at 52.5 km for the data set of *Goes et al.* [2000] are around 10^{25} Pa s indicating that at those depths the mantle can be considered predominantly elastic on timescales of glacial isostatic

adjustment, since the minimum viscosity for a viscously deforming mantle is determined at 10^{25} Pa s (Figure 4b).

4. Discussion

4.1. Large Lateral Variations in Upper Mantle Viscosity

[22] The large variations in temperature of the shallow upper mantle below Scandinavia from the thermal data sets of *Goes et al.* [2000] and *Artemieva* [2006] produce a large lateral heterogeneity of upper mantle viscosity values under Scandinavia. Estimates of viscosity variations under Scandinavia due to the lateral temperature variations reach up to three to four orders of magnitude. Due to those large variations in viscosities different parts of the upper mantle deform by different deformation mechanisms (diffusion or dislocation creep). Heterogeneous upper mantle deformation in terms of strength and deformation mechanism is primarily the result of those temperature variations, with differences in the microstructural parameters such as grain size and water content only contributing as a second-order influence to the viscosity of the upper mantle. The relatively large uncertainties in the temperature estimates (100–150°C) [*Goes et al.*, 2000] and the large difference in temperature estimates between the data sets of *Goes et al.* [2000] and *Artemieva* [2006] show that caution should be taken when individual values of viscosity are taken to be representative for the upper mantle viscosity of that region. However, the average viscosity values for Scandinavia or the variations in average viscosity between two larger areas within Scandinavia (e.g., central Finland in comparison with southwest Norway) are most likely robust estimates of the upper mantle viscosity.

[23] In the viscosity modeling of this study we have chosen to use the self-consistent olivine dislocation creep and diffusion creep flow laws from *Hirth and Kohlstedt* [2003]. *Hirth and Kohlstedt* [2003] review the various experimental data sets for olivine and provide flow laws for dislocation and diffusion creep that also include the dependences of the strain rate on water content and melt content. In recent years, those flow laws have been widely used to model the deformation behavior of olivine, and because of those reasons we have chosen to also use the flow laws of *Hirth and Kohlstedt* [2003]. The use of another flow law, e.g., using a recent dislocation creep flow law for fine-grained olivine [*Faul et al.*, 2011], would change the outcomes of the viscosities for the shallow upper mantle below Scandinavia. However, it is expected that such other flow laws would also produce changes in dominant deformation mechanism with a change in grain size, stress level and water content as is seen in Figure 5, although the exact condition at which this change occurs might vary somewhat.

4.2. Sensitivity of the Dominant Deformation Mechanism to Microstructure

[24] The outcomes of the viscosity modeling show that whether diffusion creep or dislocation creep dominates the deformation of the upper mantle below Scandinavia is very sensitive to the microstructural parameters grain size and water content as well as the stress levels present during deformation (Figures 5–8). At small grain sizes (e.g., 4 mm) and small stress levels in a dry upper mantle diffusion creep deformation dominates, but toward larger grain sizes, stress levels and water content dislocation creep becomes the dominating deformation mechanism within the upper mantle. Similarly, pressure conditions also influence which deformation mechanism is most active with an increasing contribution of dislocation creep at larger depths. This is due to the different pressure sensitivities resulting from different activation volumes within the flow laws for diffusion and dislocation creep (Table 1). It can be concluded that within the Scandinavian upper mantle both diffusion creep and dislocation creep are simultaneously active across the range of temperature, pressure, grain size and water content investigated in this study. This advocates that composite rheologies ($\dot{\varepsilon}_{total} = \dot{\varepsilon}_{diff} + \dot{\varepsilon}_{disl}$) should be used in glacial isostatic adjustments studies for Scandinavia or in studies of plate tectonic processes such as mantle convection or subduction. Studies using only diffusion creep or dislocation creep rheologies neglect the influence of the other deformation mechanism thereby potentially producing biased estimates of the viscosity of the upper mantle.

[25] Regions where dislocation creep is the dominant deformation mechanism (Figure 5) are in theory regions where seismic anisotropy should be present. However, during GIA timescales the amount of strain is too small to form strong seismic anisotropies or change or destroy the earlier formed anisotropic structure of the mantle. Therefore, the seismic anisotropy in the Scandinavian upper mantle is most likely the result of earlier tectonic events and our maps driven by GIA stress cannot be used to predict regions of seismic anisotropy. However,

stress conditions during tectonic events or during mantle convection are in the range of ~1 to several tens of MPa [e.g., *Schmeling*, 1987; *Ranalli*, 1995; *Steinberger et al.*, 2001; *Kneller et al.*, 2005], and thus do not differ significantly from stress conditions during GIA (0–30 MPa in this study). If temperature conditions are also similar, dislocation creep-dominated wet upper mantle in our study also predicts the presence of seismic anisotropy in the upper mantle of Scandinavia during earlier tectonic events.

[26] Larger contributions of diffusion creep to the deformation, and hence an absence of seismic anisotropy, can only be achieved in two cases. First, diffusion creep would dominate when the temperature conditions during those tectonic events were significantly higher than they are nowadays. Regions with still relatively high temperatures in the upper mantle of Scandinavia due to the formation of oceanic crust during the formation of the Atlantic Ocean, e.g., west of the Norwegian coast (Figure 5), are regions were less or no seismic anisotropy is expected. Regions that had lower temperatures than present, e.g., during subduction events, would favor dislocation creep and thus lead to seismic anisotropy. Second, regions with increased probability of the absence of seismic anisotropy occur toward larger depths (200 km and more) within the upper mantle due to the increased importance of diffusion creep with depth. This is caused by the different pressure dependencies of the diffusion and dislocation creep flow laws for olivine. Within the deeper asthenospheric and convecting part of the upper mantle with stress levels for convection in the range of 1–10 MPa [*Ranalli*, 1995] it is thus predicted that seismic anisotropy is most likely absent.

4.3. Viscosity Estimates and Microstructural State of the Scandinavian Upper Mantle

[27] Mean viscosity values using the temperature data sets of *Goes et al.* [2000] and *Artemieva* [2006] predict average Scandinavian viscosities for the shallow upper mantle in excess of 10^{22} Pa s for a dry upper mantle (Figure 8). Viscosity values are significantly lower at 150 and 200 km than at 50 and 100 km due to the higher temperatures at larger depths although for certain combinations of grain size and stress levels average viscosity values are again increasing at the largest depth of 200 km due to the increased importance of the pressure. At the largest depth, the temperature dependence of the viscosity is overcome by the pressure dependence of the viscosity, which increases the viscosity with increasing pressure at temperatures close to the adiabatic temperature of the upper mantle (equation (2)). Average viscosities across the depth range investigated in this study (Figure 8) show that grain sizes need to be sub-mm sized to obtain viscosities around 10^{20} Pa s in a dry upper mantle. Average viscosities using temperatures from *Goes et al.* [2000] in a wet upper mantle are in the range of 10^{19}–10^{22} Pa s, depending on depth, olivine grain sizes, stress levels and water contents (Figure 8). The time-dependent stress changes during glacial isostatic adjustment produces variations in mean viscosities for the upper mantle of Scandinavia of up to two orders of magnitude. Mean viscosity estimates reported here are similar to estimates for upper mantle viscosities under Scandinavia from glacial isostatic adjustment studies [*Lambeck et al.*, 1998; *Milne et al.*, 2001; *Steffen et al.*, 2006] or from global isostatic adjustment studies [*Peltier*, 1998]. Those studies predict viscosities around 10^{20}–10^{21} Pa s at a depth range of around 100–200 km (Figure 9). This implies that the upper mantle below Scandinavia is most likely wet, since dry rheologies predict too high mean viscosity values. This agrees with *Schotman et al.* [2009] who found that a wet rheology best matches the upper mantle viscosities and lithospheric thicknesses obtained with GIA studies and with *Kukkonen et al.* [2003] who concluded based on the observation of fluid inclusion in the Finnish mantle xenoliths that the upper mantle under Finland is wet. The data set of *Artemieva* [2006] produces mean viscosities in excess of 10^{21} Pa s for both a dry and wet upper mantle potentially indicating that temperature estimates for the upper mantle under Scandinavia from *Artemieva* [2006] underestimate the temperatures present in the Scandinavian upper mantle. Mean viscosities in the range of 10^{20}–10^{21} Pa s using the data set of *Artemieva* [2006] can only be produced with a sub-mm olivine grain size and/or very high water content ($\gg$1000 H/10^6 Si). Indications for such small grain sizes within xenoliths or exposed peridotite bodies are absent, unless deformation is controlled by fine-grained pyroxene and garnet rich layers [*Barnhoorn et al.*, 2010]. The most likely grain size in the wet upper mantle is more difficult to constrain, because due to the dominance of dislocation creep in a wet upper mantle, average viscosities are not significantly grain size dependent, when grain sizes are larger than 1 mm as is seen in the xenoliths and peridotites.

[28] Mean viscosities determined using the temperature data sets of *Goes et al.* [2000] and

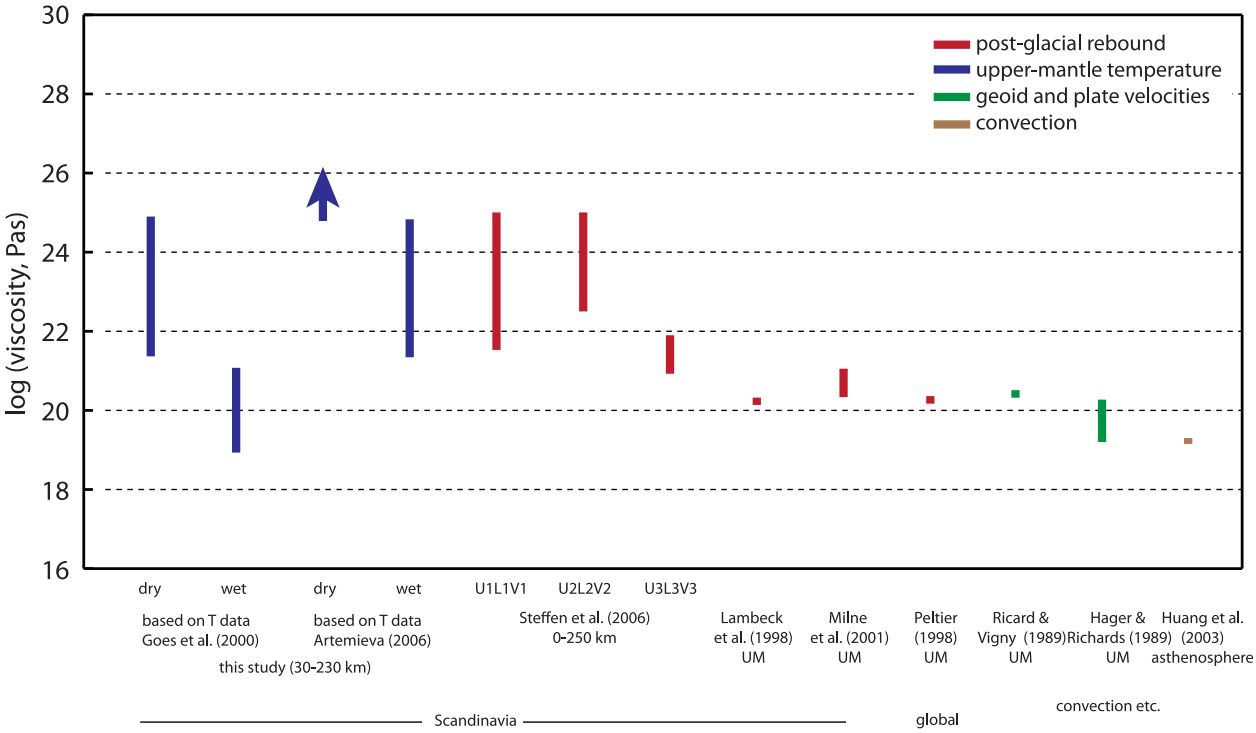

Figure 9. Comparison of viscosity estimates in this study with upper mantle viscosity estimates for Scandinavia from glacial isostatic modeling studies and global estimates from glacial isostatic adjustment, mantle convection, and geoid studies [*Ricard and Vigney*, 1989; *Hager and Richards*, 1989; *Huang et al.*, 2003].

Artemieva [2006] only take into account the first 200 km of the upper mantle, yet olivine is stable to a depth of ~410 km where olivine transforms into the high-pressure polymorph wadsleyite. In Figure 10 a geotherm is constructed that extrapolates the average temperatures for Scandinavia up to 200 km from *Goes et al.* [2000] to 410 km with an adiabatic temperature of 1400°C. Viscosity analyses along this geotherm show that the viscosities remain relatively high ($\eta > 10^{20}$ Pa s). Therefore, a significant lowering of the mean viscosities is not expected in a dry upper mantle when the complete depth range (0–410 km) for the stability of olivine is used. An increase in viscosity with depth is even expected to occur, since the pressure dependence of the viscosity becomes increasingly important at larger depths. At depths where the geotherm approaches adiabatic temperatures (~200 km), the temperature dependence of the viscosity becomes less important than the pressure dependence of the viscosity potentially resulting in an increase in viscosity with depth. However, experimental studies have produced significant variations in the activation volume V for olivine in equation (2) that controls the pressure dependence of viscosity [*Karato*, 2010]. Therefore, until a robust value of V has been obtained, viscosity profiles within the upper mantle can deviate significantly with depth from the profiles shown in Figure 10.

[29] There are two main effects that could have produced the viscosity estimates for a dry upper mantle larger than the values predicted by glacial isostatic adjustment studies (10^{20}–10^{21} Pa s, see Figure 9). First, the role of melt has been excluded in the viscosity modeling study. A melt content of 0 has been assumed throughout the study. Experimental studies [*Hirth and Kohlstedt*, 2003; *Faul and Jackson*, 2007] show that very low melt contents already cause a significant lowering of the olivine viscosity potentially explaining the generally too high viscosity estimates in this study. Significant amounts of melt (1–4% or even more) are needed to lower the average viscosity to values in the range of 10^{20} to 10^{21} Pa s. Because the current temperatures under Scandinavia are too low to expect melting, it is unlikely that any melt is present reducing the dry upper mantle viscosity. However, in a wet upper mantle, the solidus temperatures are reduced significantly. Upper mantle temperatures under Scandinavia may potentially be high enough to cause some incipient melting, although this may not change viscosity as the

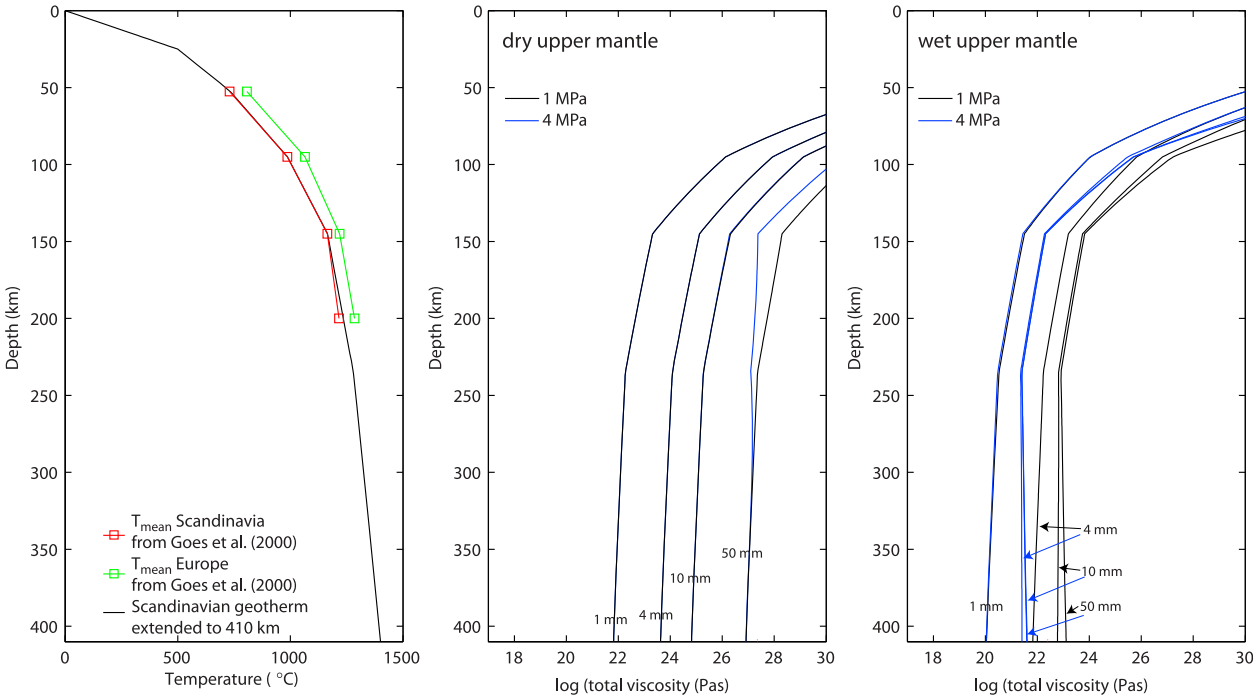

Figure 10. Viscosity profiles for a dry and wet upper mantle along a geotherm constructed from the mean Scandinavian temperatures at each depth from *Goes et al.* [2000] extended to a temperature of 1400°C at a depth of 410 km (olivine-wadsleyite transition). Viscosity profiles are produced for stress levels of 1 and 4 MPa and grain sizes of 1, 4, 10, and 50 mm.

softening caused by melting may be balanced by concentration of water into the melt [*Karato*, 1986; *Hirth and Kohlstedt*, 1996]. The presence of melt in a wet upper mantle is not needed to explain the upper mantle viscosities under Scandinavia. The effect of the presence of water alone lowers the average upper mantle viscosities to values that are in line with glacial isostatic adjustment studies. Second, it is assumed in the modeling that the main mineral olivine controls the rheology of the upper mantle and that secondary upper mantle minerals such as orthopyroxene, clinopyroxene, garnet, plagioclase or spinel do not contribute to the deformation. In mantle rocks with a heterogeneity in the distribution of the mantle minerals and in the grain size of those mantle minerals, secondary phases such as orthopyroxene or even garnet may in some instances be weaker than the dominant mineral olivine [*Skemer et al.*, 2010; *Barnhoorn et al.*, 2010]. If such heterogeneities in the mantle occur on a scale large enough to influence GIA, a reduction in the overall upper mantle viscosity may occur. The rheology of multiphase mantle rocks is poorly understood. Each individual phase may contribute proportionally to their volume occurrence in the rock (Voigt or Reuss bounds) [*Tullis et al.*, 1991; *Handy*, 1994]. The interplay between the different phases due to enhanced diffusion rates [*Bruhn et al.*, 1999] or increased grain boundary pinning may significantly alter the rheology of the multiphase aggregate.

[30] It can be concluded from the viscosity modeling using the flow laws of *Hirth and Kohlstedt* [2003] that the shallow upper mantle under Scandinavia needs to contain water to match the olivine viscosities of this study to the viscosities obtained in glacial isostatic adjustment studies. An alternative possibility in a dry upper mantle that cannot be excluded from the modeling is that the influence of secondary phases in a dry upper mantle may cause the viscosities to be lower than a dry melt-free olivine-only upper mantle.

5. Conclusions

[31] Modeling of upper mantle viscosity under Scandinavia resulted in large lateral variations in upper mantle viscosity (3–4 orders of magnitude) due to large lateral variations in temperature across Scandinavia. The time-dependent changes in stress between 30 kyr B.P. and present cause additional viscosity variations within the upper mantle of Scandinavia of 2 orders of magnitude. Using both

temperature data sets of *Goes et al.* [2000] and *Artemieva* [2006] average Scandinavian viscosities for the shallow upper mantle are predicted to be in excess of 10^{22} Pa s for a dry upper mantle and between 10^{19} and 10^{22} Pa s for a wet upper mantle, depending on olivine grain sizes, stress levels and water contents. The viscosity modeling furthermore shows that the type of upper mantle rheology (linear versus nonlinear viscous rheology) is very sensitive to the microstructural state of the upper mantle below Scandinavia. Across a realistic range of stress levels, grain sizes and water contents which can be expected to be present in the upper mantle deformation, both linear viscous diffusion creep and nonlinear viscous dislocation creep contribute to the deformation. A description of the upper mantle rheology of the shallow upper mantle should therefore consist of a composite rheology where both diffusion creep and dislocation creep contribute to the deformation ($\dot{\varepsilon}_{total} = \dot{\varepsilon}_{diff} + \dot{\varepsilon}_{disl}$). By comparing the estimates of upper mantle viscosity for Scandinavia from glacial isostatic adjustment studies (10^{20}–10^{21} Pa s) [e.g., *Lambeck et al.*, 1998; *Milne et al.*, 2001] with the average viscosities under Scandinavia of this study, it is predicted that the Scandinavian mantle is most likely wet. Mean upper mantle viscosities using the temperature data set of *Goes et al.* [2000] for a wet upper mantle (C_{OH} = 1000 H/10^6 Si) predict viscosity values in the range of 10^{19}–10^{21} Pa s across the range of grain sizes and stress levels. A dry upper mantle produces viscosity values in excess of 10^{22} Pa s. A dry upper mantle will only produce viscosities in the range of 10^{20}–10^{21} Pa s when melt was present in the upper mantle reducing the viscosity, or when upper mantle rheologies are affected by other mantle minerals thereby reducing the upper mantle viscosity.

Acknowledgments

[32] Saskia Goes and Irina Artemieva generously provided us with their thermal data sets of the upper mantle under Europe. Mark-Willem Jansen is thanked for providing his improved normal mode codes. Detailed reviews of Patrick Wu who suggested the improvement of modeling the stress evolution during GIA and an anonymous reviewer significantly improved the paper. Financial support from the Netherlands Organisation for Scientific Research (NWO) and TOPO-EUROPE is acknowledged.

References

Artemieva, I. M. (2006), Global 1° × 1° thermal model TC1 for the continental lithosphere: Implications for lithosphere secular evolution, *Tectonophysics*, *416*, 245–277, doi:10.1016/j.tecto.2005.11.022.

Artemieva, I. M., and W. D. Mooney (2001), Thermal structure and evolution of Precambrian lithosphere: A global study, *J. Geophys. Res.*, *106*, 16,387–16,414, doi:10.1029/2000JB900439.

Ave Lallemant, H. G., J.-C. C. Mercier, N. L. Carter, and J. V. Ross (1980), Rheology of the upper mantle: Inferences from peridotite xenoliths, *Tectonophysics*, *70*, 85–113, doi:10.1016/0040-1951(80)90022-0.

Barnhoorn, A., M. R. Drury, and H. L. M. van Roermund (2010), Evidence for low viscosity garnet-rich layers in the upper mantle, *Earth Planet. Sci. Lett.*, *289*, 54–67, doi:10.1016/j.epsl.2009.10.028.

Bijwaard, H., W. Spakman, and E. R. Engdahl (1998), Closing the gap between regional and global travel time tomography, *J. Geophys. Res.*, *103*, 30,055–30,078, doi:10.1029/98JB02467.

Brey, G. P., and T. Köhler (1990), Geothermobarometry in four-phase lherzolites II. New thermobarometers, and practical assessment of existing thermobarometers, *J. Petrol.*, *31*, 1353–1378.

Bruhn, D. F., D. L. Olgaard, and L. N. Dell'Angelo (1999), Evidence for enhanced deformation in two-phase rocks: Experiments on the rheology of calcite-anhydrite aggregates, *J. Geophys. Res.*, *104*, 707–724, doi:10.1029/98JB02847.

Faul, U. H., and I. Jackson (2005), The seismological signature of temperature and grain size variations in the upper mantle, *Earth Planet. Sci. Lett.*, *234*, 119–134, doi:10.1016/j.epsl.2005.02.008.

Faul, U. H., and I. Jackson (2007), Diffusion creep of dry, melt-free olivine, *J. Geophys. Res.*, *112*, B04204, doi:10.1029/2006JB004586.

Faul, U. H., J. D. Fitz Gerald, R. J. M. Farla, R. Ahlefeldt, and I. Jackson (2011), Dislocation creep of fine-grained olivine, *J. Geophys. Res.*, *116*, B01203, doi:10.1029/2009JB007174.

Franz, L., G. P. Brey, and M. Okrusch (1996), Steady state geotherm, thermal disturbances, and tectonic development of the lower lithosphere underneath the Gibeon Kimberlite Province, Namibia, *Contrib. Mineral. Petrol.*, *126*, 181–198, doi:10.1007/s004100050243.

Goes, S., R. Govers, and P. Vacher (2000), Shallow mantle temperatures under Europe from P and S wave tomography, *J. Geophys. Res.*, *105*, 11,153–11,169, doi:10.1029/1999JB900300.

Hager, B. H., and M. A. Richards (1989), Long-wavelength variations in Earth's geoid: Physical models and dynamical implications, *Philos. Trans. R. Soc. London A*, *328*, 309–327, doi:10.1098/rsta.1989.0038.

Handy, M. R. (1994), Flow laws for rocks containing two non-linear viscous phases: A phenomenological approach, *J. Struct. Geol.*, *16*, 287–301, doi:10.1016/0191-8141(94)90035-3.

Hirth, G., and D. L. Kohlstedt (1996), Water in the oceanic upper mantle: Implications for rheology, melt extraction and the evolution of the lithosphere, *Earth Planet. Sci. Lett.*, *144*, 93–108, doi:10.1016/0012-821X(96)00154-9.

Hirth, G., and D. L. Kohlstedt (2003), Rheology of the upper mantle and the mantle wedge: A view from experimentalists, in *Inside the Subduction Factory*, *Geophys. Monogr. Ser.*, vol. 138, edited by J. Eiler, pp. 83–105, AGU, Washington, D. C.

Huang, J., S. Zhong, and J. van Hunen (2003), Controls on sublithospheric small-scale convection, *J. Geophys. Res.*, *108*(B8), 2405, doi:10.1029/2003JB002456.

Ivins, E. R., and C. G. Sammis (1995), On lateral viscosity contrast in the mantle and the rheology of low-frequency geodynamics, *Geophys. J. Int.*, *123*, 305–322, doi:10.1111/j.1365-246X.1995.tb06856.x.

Jordan, T. H. (1979), Mineralogies, densities and seismic velocities of garnet lherzolites and their geophysical implications, in *The Mantle Sample: Inclusions in Kimberlites and Other Volcanics*, edited by F. R. Boyd and H. O. A. Myer, pp. 1–14, AGU, Washington, D. C.

Karato, S. (1986), Does partial melting reduce the creep strength of the upper mantle?, *Nature*, *319*, 309–310, doi:10.1038/319309a0.

Karato, S.-I. (2003), Mapping water content in Earth's upper mantle, in *Inside the Subduction Factory*, *Geophys. Monogr. Ser.*, vol. 138, edited by J. Eiler, pp. 135–152, AGU, Washington, D. C.

Karato, S.-I. (2010), Rheology of the deep upper mantle and its implications for the preservation of the continental roots: A review, *Tectonophysics*, *481*, 82–98, doi:10.1016/j.tecto.2009.04.011.

Klemann, V., and D. Wolf (1998), Modelling of stresses in the Fennoscandian lithosphere induced by Pleistocene glaciations, *Tectonophysics*, *294*, 291–303, doi:10.1016/S0040-1951(98)00107-3.

Kneller, E. A., P. E. van Keken, S.-I. Karato, and J. Park (2005), B-type olivine fabric in the mantle wedge: Insights from high-resolution non-Newtonian subduction zone models, *Earth Planet. Sci. Lett.*, *237*, 781–797, doi:10.1016/j.epsl.2005.06.049.

Kukkonen, I. T., and P. Peltonen (1999), Xenolith-controlled geotherm for the central Fennoscandian Shield: Implications for lithosphere–asthenosphere relations, *Tectonophysics*, *304*, 301–315, doi:10.1016/S0040-1951(99)00031-1.

Kukkonen, I. T., K. A. Kinnunen, and P. Peltonen (2003), Mantle xenoliths and thick lithosphere in the Fennoscandian Shield, *Phys. Chem. Earth*, *28*, 349–360.

Lambeck, K., C. Smither, and P. Johnston (1998), Sea level change, glacial rebound and mantle viscosity for northern Europe, *Geophys. J. Int.*, *134*, 102–144, doi:10.1046/j.1365-246x.1998.00541.x.

Latychev, K., J. X. Mitrovica, J. Tromp, M. E. Tamisiea, D. Komatitsch, and C. C. Christara (2005), Glacial isostatic adjustment on 3-D Earth models: A finite-volume formulation, *Geophys. J. Int.*, *161*, 421–444, doi:10.1111/j.1365-246X.2005.02536.x.

Leitch, A. M., and D. A. Yuen (1989), Internal heating and thermal constraints on the mantle, *Geophys. Res. Lett.*, *16*, 1407–1410, doi:10.1029/GL016i012p01407.

Marquering, H., and R. Snieder (1996), Shear-wave velocity structure beneath Europe, the northeastern Atlantic and western Asia from waveform inversion including surface-wave mode coupling, *Geophys. J. Int.*, *127*, 283–304, doi:10.1111/j.1365-246X.1996.tb04720.x.

Martinec, Z., and D. Wolf (2005), Inverting the Fennoscandian relaxation-time spectrum in terms of an axisymmetric viscosity distribution with a lithospheric root, *J. Geodyn.*, *39*, 143–163, doi:10.1016/j.jog.2004.08.007.

Mercier, J.-C. C., D. A. Anderson, and N. L. Carter (1977), Stress in the lithosphere: Inferences from steady state flow of rocks, *Pure Appl. Geophys.*, *115*, 199–226, doi:10.1007/BF01637104.

Milne, G. A., J. L. Davis, J. X. Mitrovica, H.-G. Scherneck, J. M. Johansson, M. Vermeer, and H. Koivula (2001), Space-geodetic constraints on glacial isostatic adjustment in Fennoscandia, *Science*, *291*, 2381–2385, doi:10.1126/science.1057022.

Paulson, A., S. Zhong, and J. Wahr (2005), Modelling post-glacial rebound with lateral viscosity variations, *Geophys. J. Int.*, *163*, 357–371.

Peltier, W. R. (1998), Post-glacial variations in the level of the sea: Implications for climate dynamics and solid earth geophysics, *Rev. Geophys.*, *36*, 603–689.

Peltier, W. R. (2004), Global glacial isostasy and the surface of the ice-age Earth: ICE-5G (VM2) model and GRACE, *Annu. Rev. Earth Planet. Sci.*, *32*, 111–149, doi:10.1146/annurev.earth.32.082503.144359.

Ranalli, G. (1995), *Rheology of the Earth*, 436 pp., Chapman and Hall, London.

Ricard, Y., and C. Vigny (1989), Mantle dynamics with induced plate tectonics, *J. Geophys. Res.*, *94*, 17,543–17,559, doi:10.1029/JB094iB12p17543.

Schmeling, H. (1987), On the interaction between small- and large-scale convection and postglacial rebound flow in a power-law mantle, *Earth Planet. Sci. Lett.*, *84*, 254–262, doi:10.1016/0012-821X(87)90090-2.

Schotman, H. H. A., L. L. A. Vermeersen, P. Wu, M. R. Drury, and J. H. P. de Bresser (2009), Constraints on shallow low viscosity zones in Northern Europe from future GOCE gravity data, *Geophys. J. Int.*, *178*, 65–84, doi:10.1111/j.1365-246X.2009.04160.x.

Shapiro, N. M., and M. H. Ritzwoller (2004), Thermodynamic constraints on seismic inversions, *Geophys. J. Int.*, *157*, 1175–1188, doi:10.1111/j.1365-246X.2004.02254.x.

Skemer, P., J. M. Warren, P. B. Kelemen, and G. Hirth (2010), Microstructural and rheological evolution of a mantle shear zone, *J. Petrol.*, *51*, 43–53, doi:10.1093/petrology/egp057.

Spengler, D., H. L. M. Van Roermund, M. R. Drury, L. Ottolini, P. R. D. Mason, and G. R. Davies (2006), Deep origin and hot melting of an Archaean orogenic peridotite massif in Norway, *Nature*, *440*, 913–917, doi:10.1038/nature04644.

Spengler, D., H. K. Brueckner, H. L. M. van Roermund, M. R. Drury, and P. R. D. Mason (2009), Long-lived, cold burial of Baltica to 200 km depth, *Earth Planet. Sci. Lett.*, *281*, 27–35, doi:10.1016/j.epsl.2009.02.001.

Steffen, H., G. Kaufmann, and P. Wu (2006), Three-dimensional finite-element modeling of the glacial isostatic adjustment in Fennoscandia, *Earth Planet. Sci. Lett.*, *250*, 358–375, doi:10.1016/j.epsl.2006.08.003.

Steinberger, B., H. Schmeling, and G. Marquart (2001), Large-scale lithospheric stress field and topography induced by global mantle circulation, *Earth Planet. Sci. Lett.*, *186*, 75–91, doi:10.1016/S0012-821X(01)00229-1.

Tullis, T. E., F. G. Horowitz, and J. Tullis (1991), Flow laws of polyphase aggregates from end-member flow laws, *J. Geophys. Res.*, *96*, 8081–8096, doi:10.1029/90JB02491.

Turcotte, D. L., and G. Schubert (2002), *Geodynamics*, 2nd ed., 456 pp., Cambridge Univ. Press, Cambridge, U. K.

Tushingham, A., and W. R. Peltier (1991), ICE-3G: A new global model of late Pleistocene deglacation based upon geophysical predictions of post-glacial relative sea level change, *J. Geophys. Res.*, *96*, 4497–4523, doi:10.1029/90JB01583.

van der Wal, W., P. Wu, H. Wang, and M. G. Sideris (2010), Composite rheology in glacial isostatic adjustment modeling, *J. Geodyn.*, *50*(1), 38–48, doi:10.1016/j.jog.2010.01.006.

Van Roermund, H. L. M., M. R. Drury, A. Barnhoorn, and A. A. de Ronde (2000), Super-silicic garnet microstructures from an orogenic garnet peridotite, evidence for an ultradeep (>6 GPa) origin, *J. Metamorph. Geol.*, *18*, 135–147, doi:10.1046/j.1525-1314.2000.00251.x.

Vermeersen, L. L. A., and R. Sabadini (1997), A new class of stratified viscoelastic models by analytical techniques, *Geophys. J. Int.*, *129*, 531–570, doi:10.1111/j.1365-246X.1997.tb04492.x.

Wang, H., and P. Wu (2006), Effects of lateral variations in lithospheric thickness and mantle viscosity on glacially induced surface motion on a spherical, self-gravitating Maxwell Earth, *Earth Planet. Sci. Lett.*, *244*, 576–589, doi:10.1016/j.epsl.2006.02.026.

Wu, P., and W. van der Wal (2003), Postglacial sealevels on a spherical, self-gravitating viscoelastic earth: Effects of lateral viscosity variations in the upper mantle on the inference of viscosity contrasts in the lower mantle, *Earth Planet. Sci. Lett.*, *211*, 57–68, doi:10.1016/S0012-821X(03)00199-7.

Zhong, S., A. Paulson, and J. Wahr (2003), Three-dimensional finite-element modelling of Earth's viscoelastic deformation: Effects of lateral variations in lithospheric thickness, *Geophys. J. Int.*, *155*, 679–695, doi:10.1046/j.1365-246X.2003.02084.x.